

# Benthic habitat mapping using high-resolution UAV imagery: A case study of Mantanani Besar Island, Sabah

Wei Sheng Chong<sup>#</sup>, Izz Khalisah Nashir, Imelus Nius,  
Pei Zhao Liew, Fikri Akmal Khodzori,  
Muhammad Aiman Mohd Azseri, Muhammad Dawood Shah

Higher Institution Centre of Excellence (HiCOE), Institut Marin Borneo, Universiti Malaysia Sabah, Jalan UMS, 88400 Kota Kinabalu, Sabah, MALAYSIA.  
<sup>#</sup> Corresponding author. E-Mail: chong@ums.edu.my; Tel: +6014-2651802.

**ABSTRACT** Precise benthic habitat mapping is essential for the efficient management and preservation of tropical marine ecosystems. This study assesses the effectiveness of Unmanned Aerial Vehicle (UAV) technology for high-resolution mapping of the benthic habitats adjacent to Mantanani Besar Island, Malaysia. Employing a Support Vector Machine (SVM) algorithm, high-spatial-fidelity imagery (GSD = 3.72 cm/pixel) was classified into two hierarchical tiers: a binary Level 1 (L1) scheme (live coral and non-living substrate) and a multi-class Level 2 (L2) scheme consisting of six distinct classes (branching coral, massive coral, patch coral, sand, coral rubble, and submerged rock). The UAV-derived classification attained an Overall Accuracy (OA) of 88.60% ( $\kappa = 0.8625$ ), illustrating the efficacy of this platform for detailed habitat description. The findings reveal that live coral occupies roughly 37.55 ha (30%) of the examined area, whilst non-coral substrates, mainly sand and rubble, constitute the remaining 88.86 ha (70%). The occurrence of fragmented benthic substrates, especially in settlement locales, indicates considerable past reef degradation possibly caused by sedimentation and human activities. This study highlights the use of UAVs as a precise instrument for marine surveillance, delivering essential spatial data for the conservation of Mantanani's biodiversity.

**KEYWORDS:** Benthic habitat mapping; Drone; Pulau Mantanani Classification; Borneo

Received 27 February 2026 Revised 23 March 2026 Accepted 27 March 2026 In press 28 March 2026 Online 29 March 2026

© Transactions on Science and Technology

Original Article

## INTRODUCTION

Coral reefs constitute highly productive and biologically diversified ecosystems, serving as critical indices of marine health and underpinning worldwide marine resource production (Wilkinson, 2008). Nonetheless, these ecosystems have undergone significant degradation in recent decades due to human-induced disturbances and global climate change. The rise in global temperatures and anomalies in sea surface temperatures has exacerbated coral bleaching events, threatening the integrity of reef ecosystems (Hughes *et al.*, 2018a). On Mantanani Island, these fragile ecosystems are progressively jeopardised by the interaction of many stressors and fluctuating local environmental conditions. Consequently, the development of dependable mapping and monitoring methodologies is essential for recording habitat extent and guiding restoration and management initiatives (Andréfouët *et al.*, 2001; Green *et al.*, 2000; Mumby *et al.*, 1999).

Ongoing challenges, such as elevated acquisition costs for sub-meter datasets, prolonged revisit intervals, and substantial atmospheric interference due to cloud cover—especially in tropical regions—persistently hinder the utilisation of orbital sensors for ultra-fine-scale ecological research, potentially jeopardising the mapping of shallow-water benthic ecosystems (Ventura *et al.*, 2023). UAV platforms rectify these shortcomings by functioning at low altitudes, allowing sensors to obtain imagery with a centimetre-scale ground sampling distance (GSD) at viable and competitive costs (Castellanos-Galindo *et al.*, 2019). This elevated precision enables the identification of nuanced spatial patterns and minute variations in coral health—such as bleaching incidents intensified by

climate change and sea surface temperature anomalies – which are crucial for formulating evidence-based conservation policies. Moreover, UAV utilisation bypasses the temporal and logistical limitations inherent in satellite scheduling, delivering 'on-demand' data that accurately represents prevailing ecological conditions (Colomina & Molina, 2014; Pajares, 2015). The incorporation of UAV-based mapping signifies a significant progression in habitat monitoring, biodiversity assessment, and ecosystem management, establishing it as an essential instrument for the high-resolution documentation of diverse shallow-water reef systems (Casella *et al.*, 2016, Casella *et al.*, 2017; Hamylton, 2011; Muslim *et al.*, 2019).

While satellite-based habitat mapping is a well-established technology, its efficacy is often limited by insufficient spatial resolution and atmospheric disturbances. The authors' previous research built the technological foundation for tackling these difficulties by developing the Theil-Sen regression glint correction (TSGC) and a seed pixel region growth methodology (Chong *et al.*, 2021). Research at Bidong Island demonstrated that accounting for specular reflection can improve coral classification accuracy by 25.6% compared to uncorrected datasets. The authors have investigated the broader synergy between remote sensing and marine invasion science, advocating for the utilisation of high-resolution sensors on UAVs to link conventional orbital platforms with field monitoring for biological invasions (Chong *et al.*, 2023).

This study employs these methodological and conceptual foundations specifically on Mantanani Besar Island. This research provides a precise, location-specific baseline, unlike the computational focus of the 2021 study and the review-orientated approach of the 2023 work. This study utilises a two-tier hierarchical classification scheme (Level 1 binary and Level 2 multi-class) to evaluate ultra-fine-scale imagery (GSD = 3.72 cm/pixel) for characterising live coral distribution and identifying specific anthropogenic stressors in the Mantanani Archipelago. This research seeks to establish an effective hierarchical classification framework to produce accurate, multi-class benthic habitat maps, which will serve as a foundation for long-term ecosystem monitoring and informed conservation efforts.

## METHODOLOGY

### Study Site

The Mantanani Archipelago, located off the northwestern coast of Sabah, Malaysia, consists of three islands: Mantanani Besar, Mantanani Kecil, and Lingisan. This study focuses on Mantanani Besar, the group's largest island, with a land area of about 188.1 hectares. The island is surrounded by diverse marine ecosystems, including seagrass meadows and coral reef complexes. During a four-day UAV survey campaign, data was collected from eleven different sites along the coastline adjacent to JSK Mantanani Beach. Figure 1 depicts the geographical distribution of these study sites and the flight trajectories used to collect high-resolution imagery.

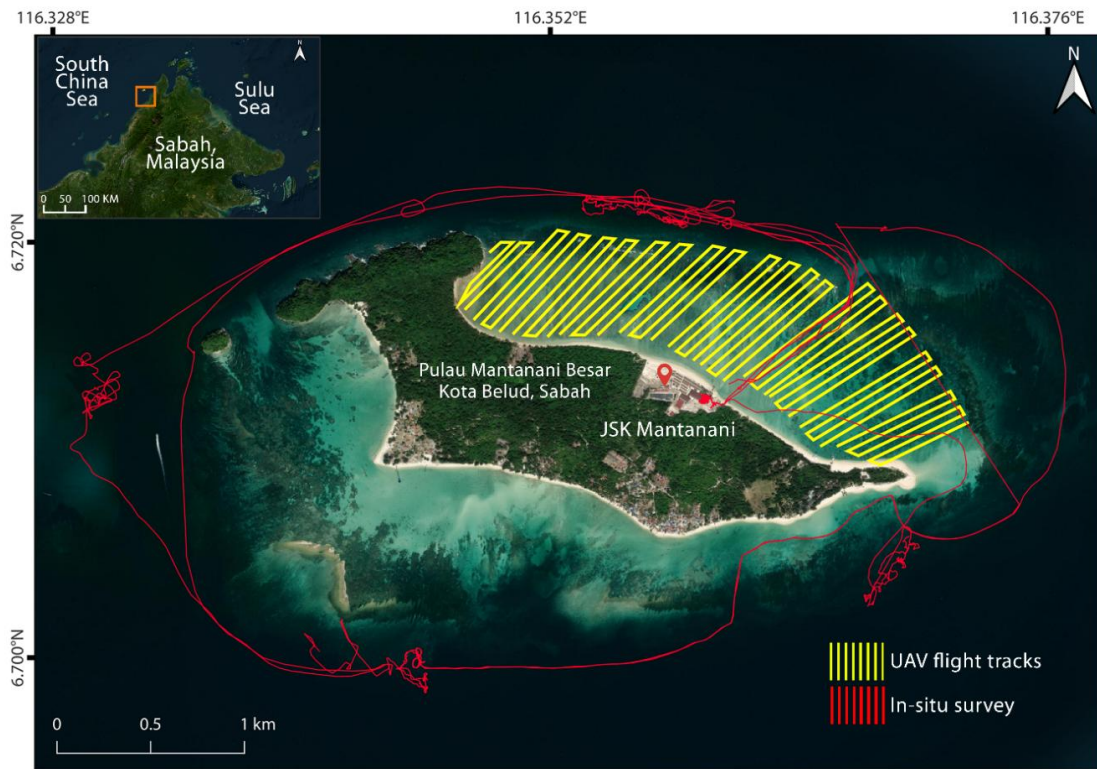


**Figure 1.** Geographical location of Mantanani Besar Island, Sabah, illustrating the UAV flight trajectories and concurrent in situ ground-truthing survey transects.

### UAV Data Collection

UAV surveys were performed at eleven study sites along the shoreline of JSK Mantanani Beach, Sabah, Malaysia, from 6 to 9 November 2024. To alleviate the impacts of sun glint and specular reflection on the sea surface, all UAV missions commenced at roughly 06:15 AM local time. Environmental variables, encompassing meteorological and tidal conditions during the study period, are summarized in Table 1.

**Table 1.** Summary of meteorological and tidal conditions recorded during the UAV data acquisition campaign.

Environmental Characteristics	Date				Data Source
	06/11/2024	07/11/2024	08/11/2024	09/11/2024	
<b>Meteorological data</b>					
Wind direction	Southwest	Southwest	East-Northeast	West	UAV Forecast ( <a href="https://www.uavforecast.com/">https://www.uavforecast.com/</a> )
Wind speed (km/h)	10.66	15.35	12.09	7.77	
Sea surface temperature (°C)	28.6	28.6	28.8	28.8	
Atmospheric temperature (°C)	29.7	28.6	29.0	28.0	
Cloud cover (%)	86	93	91	54	
Precipitation probability (%)	3	33	1	1	
<b>Tidal data</b>					
Tidal current	0.187	0.263	0.142	0.199	Tide Forecast ( <a href="https://www.tideforecast.com/">https://www.tideforecast.com/</a> )
Lowest astronomical tide (m)	0.30	0.40	0.41	0.44	
Highest astronomical tide (m)	1.96	1.96	1.90	1.80	
Time of sunrise (AM)	06:02	06:02	06:02	06:02	
Time of sunset (PM)	17:54	17:54	17:54	17:53	

Data acquisition was conducted with a DJI Air 2S platform configured with a high-resolution CMOS sensor. The aircraft operated at a stable altitude of 120 m above sea level, resulting in a Ground Sampling Distance (GSD) of 3.72 cm/pixel. Flight missions were conducted at a ground speed of 5 m/s, with the camera positioned at a nadir angle (90°) to guarantee an ideal vertical view for benthic mapping. To ensure effective photogrammetric reconstruction and orthomosaic creation, both frontal and lateral overlaps (sidelap) were sustained above 75%.

Approximately 2,200 aerial photos were obtained during the four-day campaign. The daily operating procedure entailed visiting two to three sites per mission, with designated image counts and site-specific metadata outlined in Table 2. Figure 2 illustrates the spatial distribution of the eleven flight trajectories within the research area.

**Table 2.** Summary of the total aerial images acquired during the four-day UAV survey campaign.

Site	Date	Total photos
1, 2, 3	06/11/2024	349
4, 5, 6	07/11/2024	394
7, 8	08/11/2024	224
9, 10, 11	09/11/2024	278

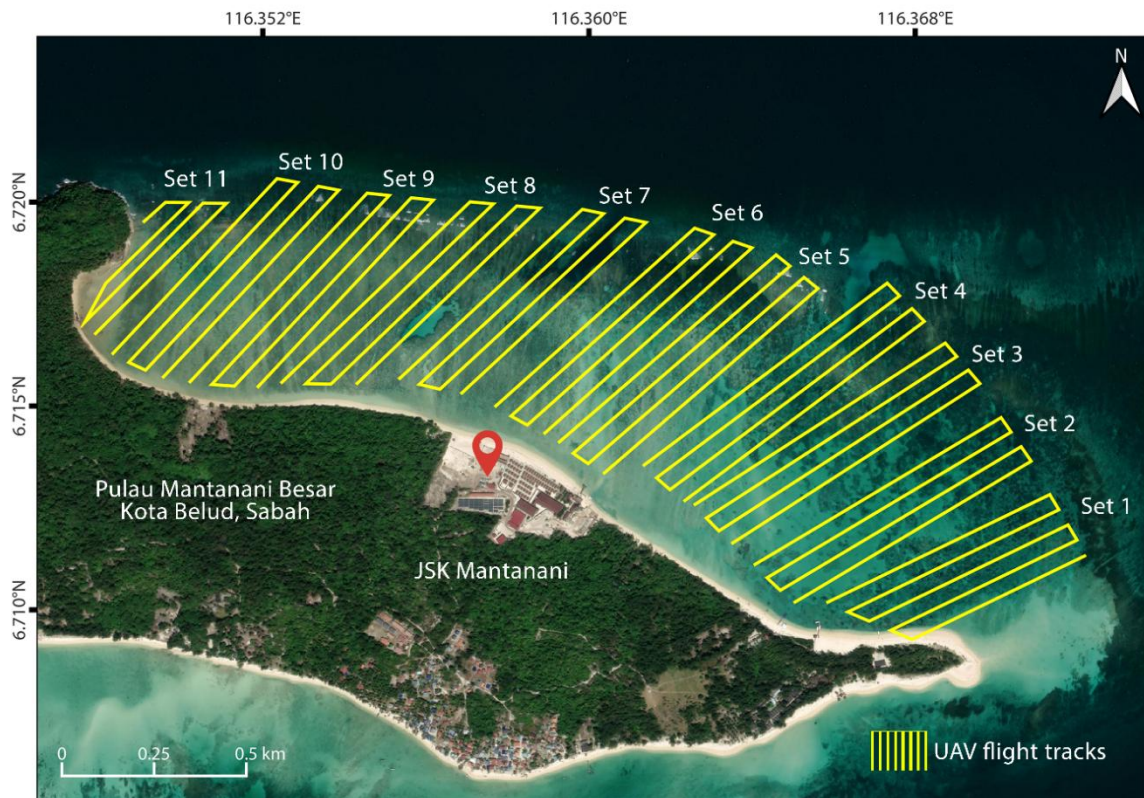


**Figure 2.** UAV flight trajectories for study sites 1–11 during the 2024 benthic mapping campaign.

### In Situ Data Acquisition and Ground-Truthing

In conjunction with the UAV surveys, a comprehensive in situ data collection campaign was conducted for providing the ground truth necessary for the calibration and validation of the remote sensing datasets. This approach involved georeferenced underwater photography, or geotagging, performed via snorkelling across the research area. This data is essential for verifying habitat attributes and enhancing the thematic accuracy of UAV imagery in complex coastal environments. Figure 3 depicts the systematic approach for in situ data collection.



**Figure 3.** Workflow for in situ validation and georeferenced underwater image acquisition (geotagging) at the research location.

During the field studies, exact GPS coordinates were documented alongside direct observations of benthic substrates, encompassing diverse coral reef morphologies and related marine environments. This thorough field validation guarantees the dependability of the ensuing remote sensing assessments and categorisation results. Illustrative examples of the underwater imagery obtained during the ground-truthing exercise are displayed in Figure 4. Ventura *et al.* (2023) emphasise that field-based geotagging is essential for validating high-resolution remote sensing products, offering vital spatial and biological context for mapping shallow-water ecosystems. Subsequent to data collecting, the in-situ observations were classified into specific habitat categories; the comprehensive descriptions and criteria for each category are given in Table 3.



**Figure 4.** Representative in situ underwater photographs illustrating different benthic habitat classes: (A) patch coral; (B) a mixture of sand, coral rubble, and branching coral; and (C) massive coral morphologies recorded during the ground-truthing survey.

**Table 3.** Classification scheme and descriptive criteria for the benthic habitat classes identified in the study area.

Benthic class	Description
Branching coral (BC)	Living corals dominated by <i>Acropora</i> exhibit a branching growth structure. This includes genera such as <i>Acropora</i> , <i>Pocillopora</i> , and <i>Porites</i> .
Massive coral (MC)	Live coral composed primarily of <i>Porites</i> exhibiting a massive or submassive growth structure. The genera represented include <i>Diploastrea</i> , <i>Favites</i> , and <i>Goniastrea</i> .
Patch coral (PC)	Living coral features a variety of forms, including branching, tabulate, foliose, massive, solitary, and encrusting species such as <i>Fungia</i> and <i>Ctenactis</i> .
Sand (S)	Fine and smooth sand without the presence of coral rubble.
Coral rubble (CR)	Fragments of dead coral that are quite loose, typically measuring less than 10 centimetres in length, can easily be swept away by the waves.
Submerged rock (R)	Rocky formations located beneath the water's surface, commonly found in shallow or intertidal areas, which may be partially or completely submerged based on tidal fluctuations.

## Marine Habitat Classification

### *Image Masking and Data Integration*

Prior to supervised classification, the orthomosaic was subjected to a preprocessing phase that included masking and data overlay. The masking procedure was utilised to eliminate unnecessary elements, including artificial structures, surface wave action, and exposed (non-submerged) rocks, from the orthomosaic. This technique was essential to eradicate spectral noise and guarantee that these features would not disrupt the benthic classification outcomes. Thereafter, the georeferenced in situ data, obtained through snorkelling at the survey sites, were layered on the orthomosaic to inform the selection of training sites. Training samples were subsequently delimited throughout the study area and classified into six separate benthic habitat categories: Sand (S), Branching Coral (BC), Massive Coral (MC), Patch Coral (PC), Submerged Rock (R), and Coral Rubble (CR).

### *Supervised Classification of UAV Imagery*

The supervised classification of the UAV-derived orthomosaic was performed using the Support Vector Machine (SVM) algorithm within the ArcMap 10.8 software. SVM, a robust machine learning classifier, was selected due to its proficiency in handling high-dimensional remote sensing data and its proven ability to achieve high thematic accuracy in complex marine environments. This algorithm categorises pixels through a multidimensional analysis of spatial, textural, and spectral properties, making it particularly effective for distinguishing heterogeneous reef habitats (Meister & Qu, 2024).

The classification output was structured according to a standardized two-tier hierarchical scheme. Level 1 (L1) comprises a broad binary classification focused on general ecosystem health, distinguishing exclusively between "live coral" and "non-living" substrates. Building upon this, the Level 2 (L2) scheme provides a high-resolution thematic map consisting of six discrete benthic classes: S, BC, MC, PC, R and CR. This hierarchical approach enables both a broad assessment of coral cover and a more detailed examination of individual community compositions.

### *Accuracy Assessment of UAV Imagery*

The thematic accuracy of the classified UAV-derived orthomosaics (GSD = 3.72 cm/pixel) was evaluated within the ArcMap 10.8 environment to determine the reliability of the benthic habitat maps. A set of independent validation points was generated, utilising the georeferenced in situ ground-truth data to ensure a rigorous comparison between the classified outputs and observed field conditions. These validation points were distinct from the training samples to avoid bias in the assessment.

Error (confusion) matrices were constructed for each classified map to quantify the correspondence between the predicted habitat classes and the reference data. From these matrices, key statistical metrics were derived, including Overall Accuracy (OA) and the Kappa coefficient ( $\kappa$ ). These indicators provide a comprehensive evaluation of the classification performance, with the Kappa coefficient specifically accounting for the agreement occurring beyond chance. Furthermore, producer's and user's accuracies were calculated for each discrete benthic category to identify specific class-level misclassifications and ensure the high-fidelity mapping required for marine ecosystem monitoring.

## RESULTS AND DISCUSSION

### UAV Orthomosaic Generation and Pre-processing

Following data acquisition, the UAV-acquired imagery was processed through a rigorous photogrammetric workflow using Agisoft Metashape (Professional Edition). This software was selected for its robust Structure-from-Motion (SfM) algorithms, which facilitate high-precision geometric and radiometric corrections. The photogrammetric reconstruction of the UAV imagery was executed through a systematic three-stage workflow. The process commenced with image alignment and the generation of a sparse point cloud to establish the spatial framework. This was followed by the reconstruction of a 3D mesh and texture to provide geometric depth and radiometric detail. The workflow culminated in the generation of a seamless, distortion-free orthomosaic, providing a geometrically accurate representation of the surveyed benthic environment at a resolution of 3.72 cm/pixel. By accounting for perspective distortions and terrain relief, the workflow produced a geometrically accurate representation of the surveyed benthic environment. The resulting orthomosaic (Figure 5) was subsequently masked to exclude extraneous non-biological features, such as surface waves and anthropogenic structures, ensuring the integrity of the subsequent supervised classification.

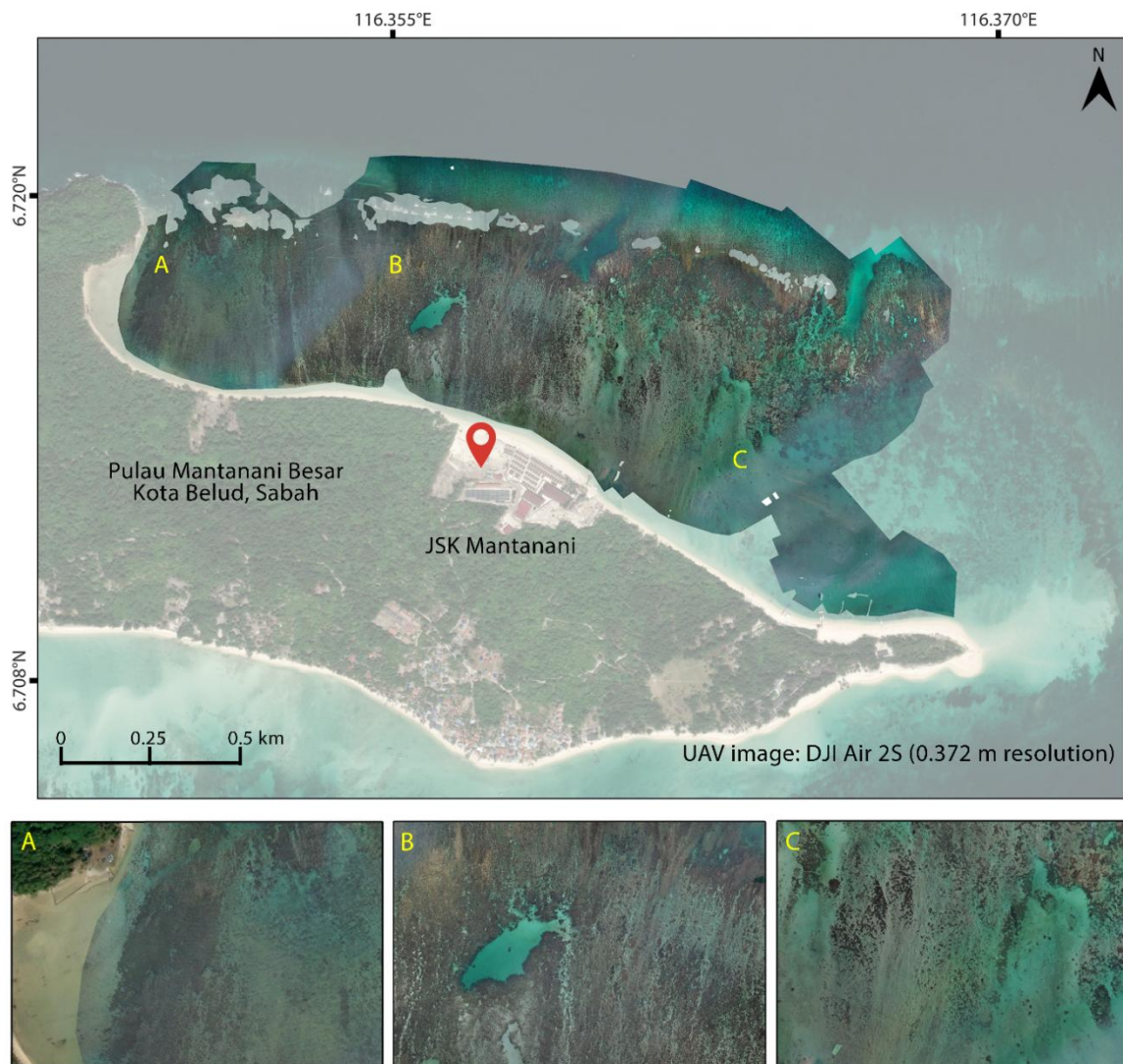


**Figure 5.** High-resolution orthomosaic of the study area with a spatial resolution of 3.72 cm/pixel generated via photogrammetric orthorectification of the UAV imagery.

To facilitate a detailed analysis, the study area was divided into three distinct sectors: Areas A, B, and C (Table 4). Area A, situated proximal to the local residential settlement, is predominantly characterised by sand substrates and submerged rock formations. In contrast, Area B is largely dominated by complex coral reef structures, primarily comprising submerged and emergent rocks and branching coral colonies. Area C represents the most extensive sandy expanse within the archipelago and features isolated seagrass patches, which serve as critical grazing habitats for sea turtle populations.

**Table 4.** Summary of site-specific characteristics and substrate descriptions for the surveyed sectors at Mantanani Island.

Area	Description
A	The village area is dominated by sand and submerged rocks; some coral is present in the area.
B	Rock and branching coral are dominant in this area. A small area of sand is present in this location.
C	This area is dominated by sand. A small area of seagrass is present, a grazing zone for turtles.

While the advancement of UAV technology has significantly enhanced the capacity for fine-scale habitat monitoring on Mantanani Besar Island, several operational constraints were identified. A primary challenge involved radiometric inconsistency caused by fluctuating illumination conditions during the multi-day data collection period. Despite initiating flights at approximately 6:15 AM to minimise sun glint, variations in cloud cover and atmospheric conditions resulted in visible spectral shifts between survey dates. As illustrated in Figure 5, these discrepancies manifest themselves as distinct colour variations across different flight sectors within the stitched orthomosaic. Such inconsistencies in spectral signatures can impede the accuracy of machine learning classifiers and diminish the visual homogeneity of the final product. Consistent lighting is a prerequisite for high-fidelity orthorectification, as it reduces projection errors and ensures a more precise digital model (Burdziakowski & Bobkowska, 2021).

### Benthic Habitat Classification and Spatial Distribution

The supervised classification and subsequent accuracy assessment were executed in ArcMap 10.8, leveraging training and validation datasets derived from georeferenced in situ observations. The field data were partitioned into a 70:30 ratio for training and validation, respectively. Training samples were delineated via manual polygon digitisation on the high-resolution orthomosaic (Figure 6), covering six discrete benthic classes. The training dataset comprised a total of 482,359 pixels, distributed across branching coral (BC;  $n = 76,577$ ), submerged rock (R;  $n = 83,830$ ), coral rubble (CR;  $n = 59,505$ ), massive coral (MC;  $n = 90,651$ ), sand (S;  $n = 94,839$ ), and patch coral (PC;  $n = 77,257$ ). Detailed descriptions of these thematic classes are provided in Table 5.

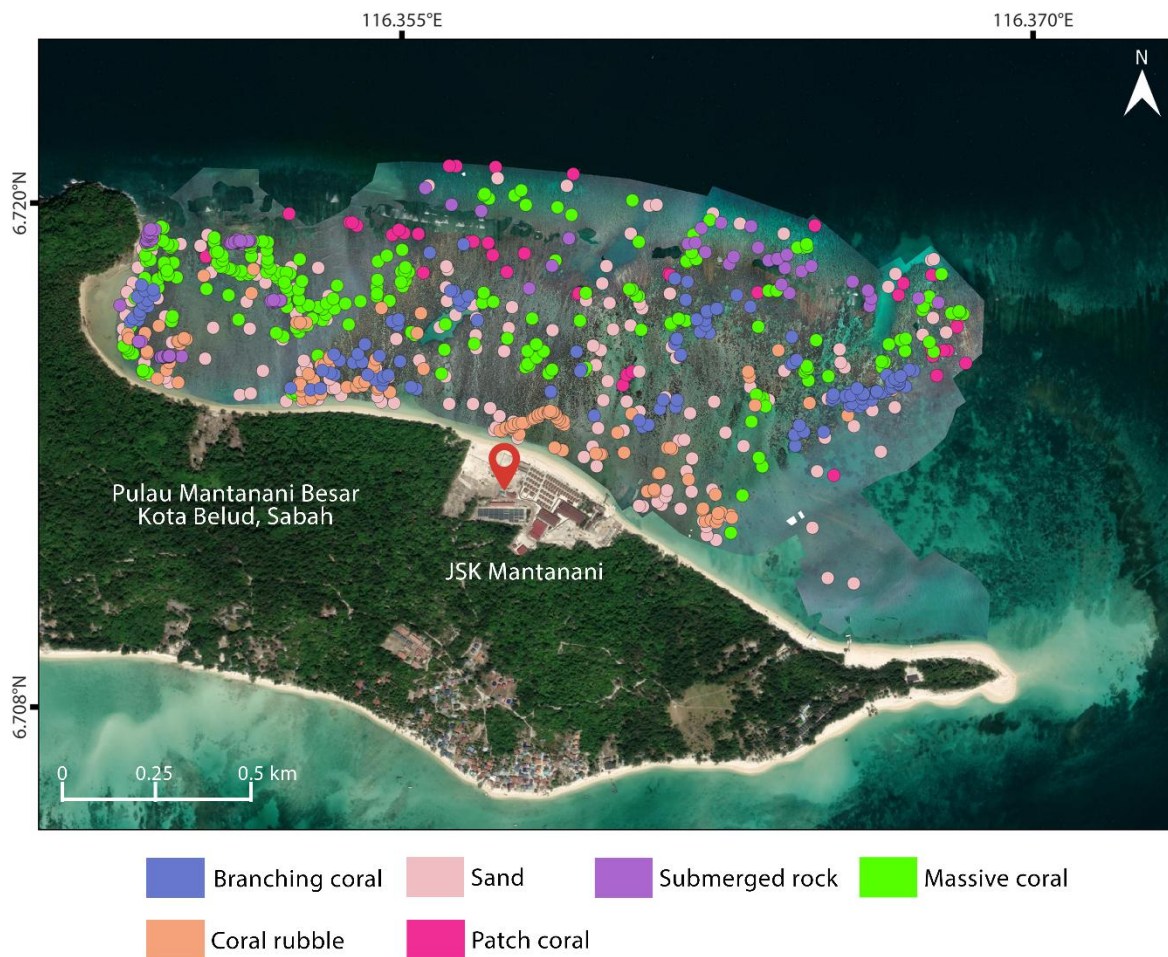


**Figure 6.** Spatial distribution of in situ ground-truth samples overlaid on the high-resolution UAV-derived orthomosaic.

**Table 5.** Thematic definitions and morphological characteristics of the benthic habitat classes identified by the UAV imagery.

Benthic class	Code	Description
Branching coral	BC	Living corals dominated by <i>Acropora</i> exhibit a branching growth structure. This includes genera such as <i>Acropora</i> , <i>Pocillopora</i> , and <i>Porites</i> .
Massive coral	MC	Live coral composed primarily of <i>Porites</i> exhibiting a massive or submassive growth structure. The genera represented include <i>Diploastrea</i> , <i>Favites</i> , and <i>Goniastrea</i> .
Patch coral	PC	Living coral features a variety of forms, including branching, tabulate, foliose, massive, solitary, and encrusting species such as <i>Fungia</i> and <i>Ctenactis</i> .
Sand	S	Fine and smooth sand without the presence of coral rubble.
Coral rubble	CR	Fragments of dead coral that are quite loose, typically measuring less than a centimeter in length, can easily be swept away by the waves.
Submerged rock	R	Rocky formations located beneath the water's surface are commonly found in shallow or intertidal areas, where they can be either partially or completely submerged based on tidal fluctuations.

The spatial distribution of the Mantanani Besar Island benthos was successfully mapped through the implementation of the SVM algorithm, with the results structured into the established hierarchical levels. The Level 1 (L1) binary output highlights a dominance of non-coral substrates, particularly in the northern and southern sectors of the study area (Figure 7), where sand and rubble are most prevalent. Specifically, the L1 classification indicates that live coral covers approximately 30% (37.55 ha) of the surveyed area, while non-coral substrates account for the remaining 70% (88.86 ha).

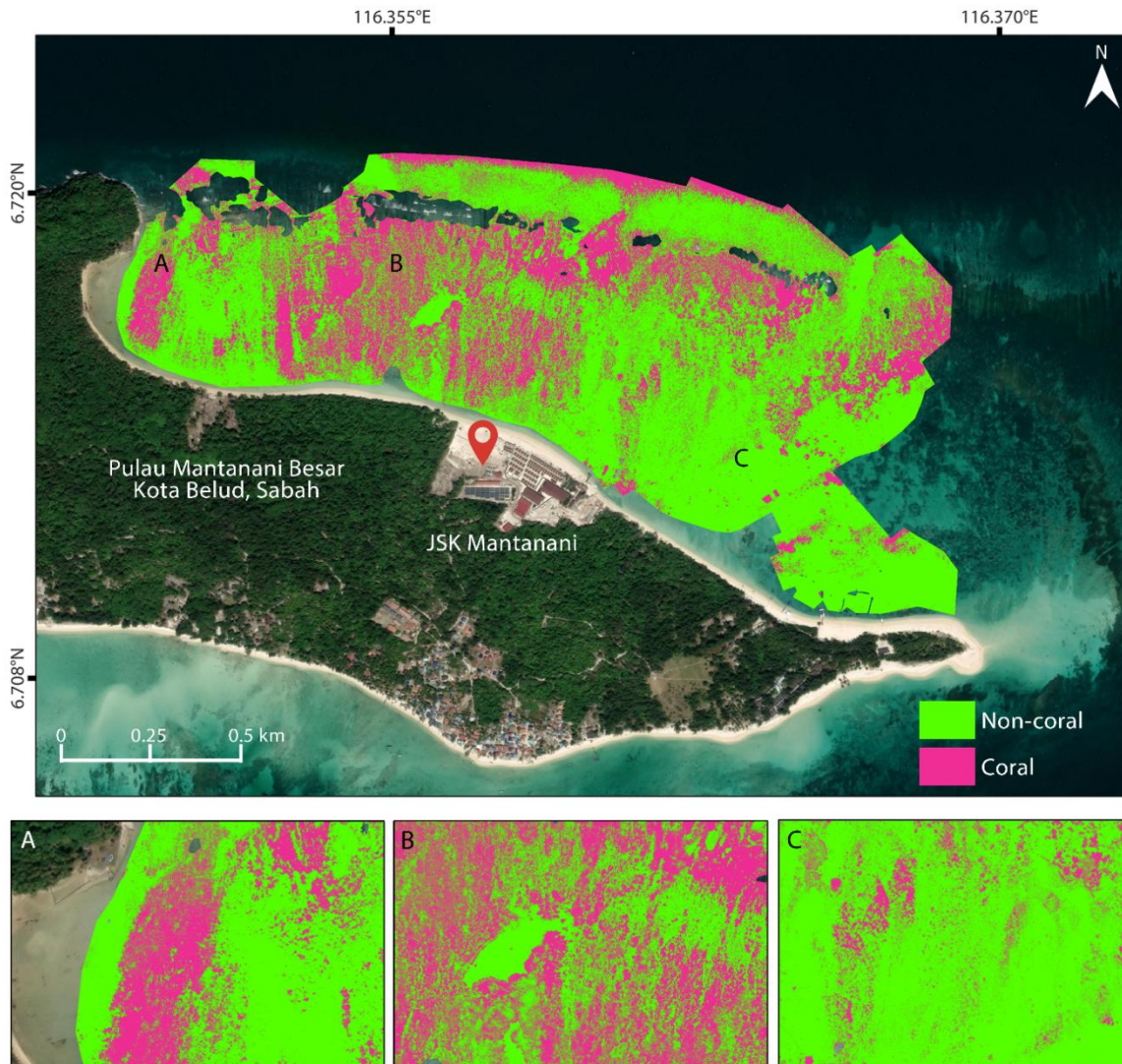


**Figure 7.** Binary (Level 1) benthic classification map illustrating the spatial distribution of live coral and non-living substrate categories across study sites 1–11.

The Level 2 (L2) multi-class thematic map provides the fine-scale detail necessary for monitoring sediment dynamics and fragmented coral structures (Figure 8). Quantitative analysis of the L2 results reveals a highly fragmented benthos where sand and coral rubble are the dominant features, covering 27% (34.37 ha) and 27% (33.60 ha) of the area, respectively. These are followed by submerged rock (16%), patch coral (11%), massive coral (10%), and branching coral (9%). This detailed composition is critical for identifying reef degradation hotspots, as the high proportion of rubble suggests significant impacts from past destructive practices or infrastructure development (Tuttle & Donahue, 2002), which may include activities such as overfishing, coastal construction, and pollution that have led to the deterioration of coral ecosystems.

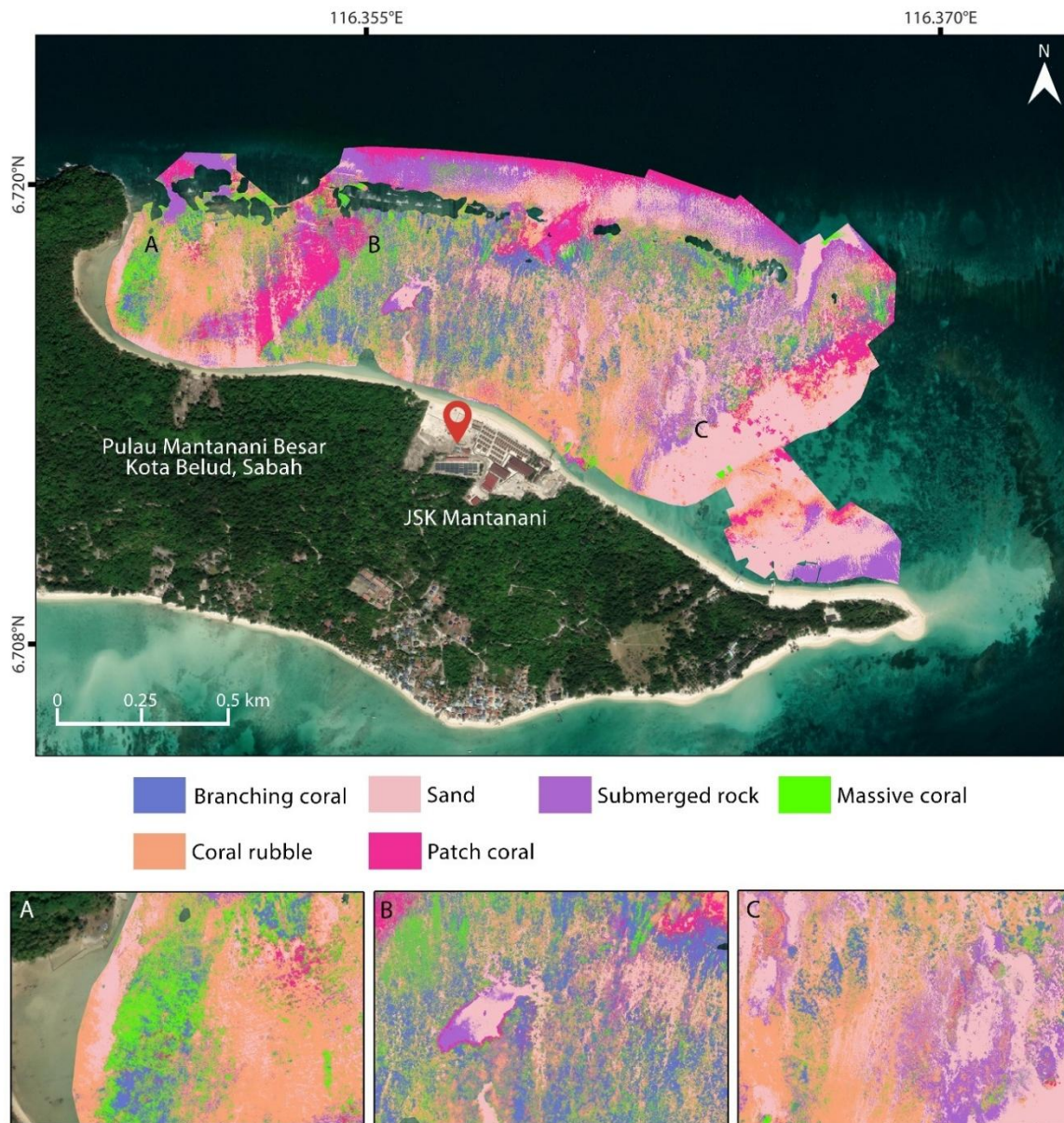


**Figure 8.** Multi-class (Level 2) benthic habitat thematic map illustrating the spatial distribution of six discrete classes across study sites 1–11.

The benthic composition of Mantanani Besar Island varies significantly across the three studied sectors. Area A, situated proximal to the local residential settlement, is predominantly characterized by non-coral elements such as sand and rubble, with massive coral (MC) serving as the primary live coral form. This prevalence of stress-tolerant corals likely reflects the anthropogenic pressures associated with the nearby village, such as pollution and habitat destruction, which can adversely affect coral health and diversity. In contrast, Area B appears to have preserved its ecological integrity, exhibiting the highest density of live coral, particularly branching (BC) and massive (MC) colonies. Finally, Area C is predominantly characterized by sandy expanses with isolated patches of seagrass, which were qualitatively identified during in situ ground-truthing. These meadows are of vital ecological importance, serving as primary grazing zones for *Chelonia mydas* (green sea turtles) and providing critical ecosystem services such as carbon sequestration and fisheries support.

While the current study confirmed the presence of these habitats, we acknowledge that quantifying seagrass density—rather than merely mapping its extent—is essential for a comprehensive evaluation of the island’s biodiversity and grazing capacity. Future research should leverage machine learning techniques, such as those proposed by Meister and Qu (2024), to derive density metrics from high-resolution UAV imagery. Such precision-based monitoring is a cornerstone of sustainable marine management practices, ensuring that fragile grazing zones are protected from the potential stressors of unregulated tourism and habitat fragmentation.

### Quantitative Benthic Composition

Statistical analysis of the L1 classification (Figure 9) indicates that live coral covers approximately 30% (37.55 ha) of the surveyed area, while non-coral substrates account for 70% (88.86 ha). This distribution reflects broader trends in Southeast Asian reef systems, where coral cover is increasingly threatened by sedimentation and human activity (Hughes *et al.* 2018b).

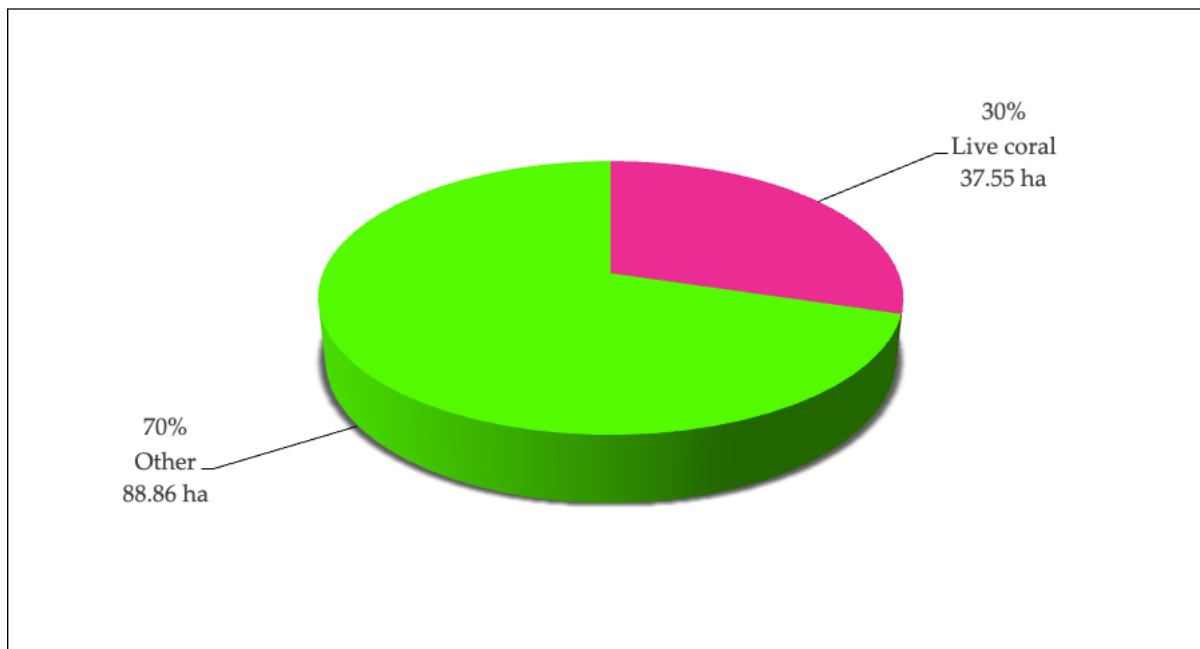


**Figure 9.** Spatial extent (ha) of benthic substrate categories derived from the Level 1 (L1) binary classification of the UAV orthomosaic.

The L2 quantitative results (Figure 10) highlight a highly fragmented benthos. Sand and coral rubble are the dominant features, covering 27% (34.37 ha) and 27% (33.60 ha), respectively. This is followed by submerged rock (16%; 20.90 ha), patch coral (11%; 13.51 ha), massive coral (10%; 12.38 ha), and branching coral (9%; 11.66 ha). While this study provides a single-period snapshot of the benthos, the high proportion of coral rubble (27%) suggests that the reef flat is currently in a state of significant fragmentation. This condition may be a legacy of historical tourism infrastructure development or past destructive fishing practices, which have contributed to the degradation of the reef ecosystem and its biodiversity. Without long-term temporal data, these findings serve as a high-resolution baseline to which future annual surveys can be compared to accurately measure degradation or recovery trends. The utility of UAVs in discerning these detailed compositions is consistent with recent findings by Stone *et al.* (2024), reinforcing the role of high-resolution remote sensing in tracking ecosystem health.

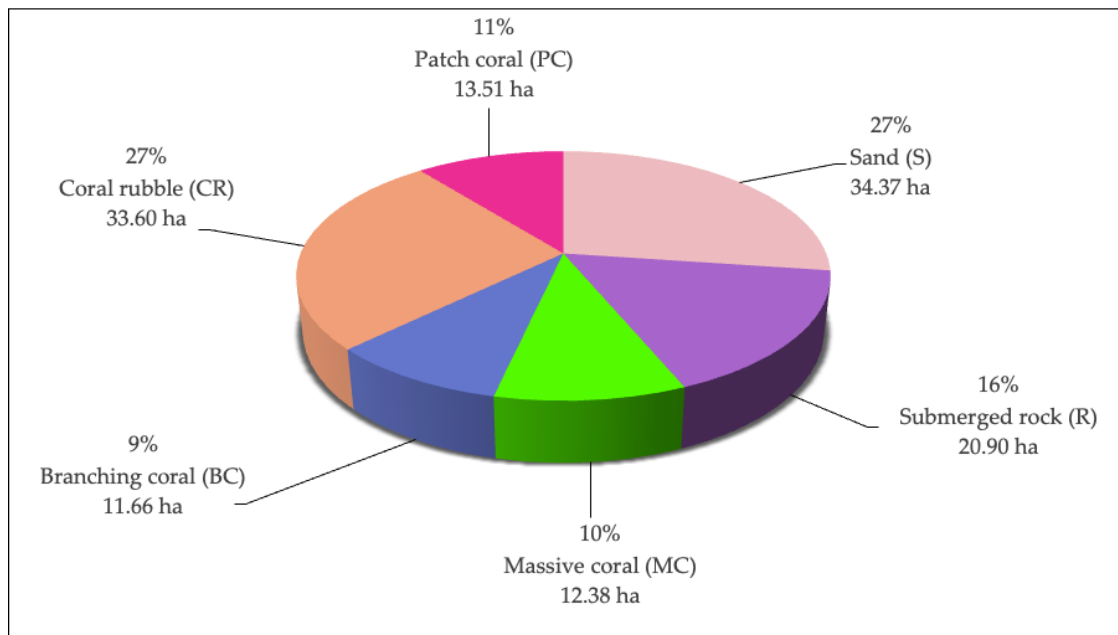


**Figure 10.** Quantitative distribution of the spatial extent (ha) for the six discrete benthic habitat classes derived from the Level 2 (L2) thematic classification.

### Accuracy Assessment

The thematic accuracy of the UAV-derived benthic habitat maps was evaluated within the ArcMap 10.8 environment through a rigorous validation process. An error matrix (confusion matrix) was generated to assess the correspondence between the classified thematic outputs and the independent in situ validation dataset, a standard procedure for quantifying the reliability of remote sensing classifications (Wu, 2022). To ensure statistical significance across the eleven study sites, a total of 144,798 validation pixels were utilised to populate the error matrix.

As presented in Table 6, the error matrix provides a comprehensive breakdown of the classification performance, identifying the specific spectral confusions between habitat classes. These data were further utilised to derive key accuracy indices, including overall accuracy (OA), producer accuracy, user accuracy, and the Kappa coefficient ( $\kappa$ ), ensuring the high-fidelity mapping required for marine ecosystem monitoring.

**Table 6.** Error (confusion) matrix for the SVM-based benthic habitat classification of the high-resolution UAV orthomosaic.

Classified	Reference							Row total	User Accuracy (%)
	Code	S	R	MC	BC	CR	PC		
Sand	S	28452	0	0	0	0	0	28452	100.00
Submerged rock	R	0	22731	1509	0	0	909	25149	90.39
Massive coral	MC	0	1472	24987	0	269	467	27195	91.88
Branching coral	BC	0	459	450	15596	441	6027	22973	67.89
Coral rubble	CR	179	707	0	2507	14459	0	17852	80.99
Patch coral	PC	0	227	664	0	225	22061	23177	95.18
Column total		28631	25596	27610	18103	15394	29464	144798	
Producer Accuracy (%)		99.37	88.81	90.5	86.15	93.93	74.87		
Overall Accuracy (%)		88.60							
Kappa coefficient		0.8625							

The error matrix and associated thematic accuracy metrics for the benthic habitat classification across Sites 1–11 are detailed in Table 6. Sand (S) achieved the highest user accuracy (UA) at 100%, followed by patch coral (PC) at 95.18%, massive coral (MC) at 91.88%, and submerged rock (R) at 90.39%. Conversely, coral rubble (CR) and branching coral (BC) exhibited lower thematic reliability, with user accuracies of 80.99% and 67.89%, respectively. The Overall Accuracy (OA) of the classification was 88.60%, with a Kappa coefficient ( $\kappa$ ) of 0.8625. According to standard remote sensing benchmarks, a  $\kappa$  value exceeding 0.80 represents "strong" or "almost perfect" agreement between the classified thematic map and the in-situ ground-truth data.

Producer accuracy (PA) ranged from 74.87% for patch coral (PC) to 99.37% for sand (S), reflecting varying levels of class-specific omission and commission errors. These results underscore the high reliability of the UAV-derived maps for sand, patch coral, and massive coral—all of which are critical indicators for reef health monitoring. However, the diminished accuracy for coral rubble and branching coral suggests significant spectral confusion between these two classes. This is likely attributable to their similar morphological structures and spectral signatures in high-resolution imagery, particularly in complex, shallow-water environments where varying water depths and turbidity can further homogenise their reflectance patterns.

### Limitations of RGB UAV Mapping

While the high-spatial-fidelity imagery (GSD = 3.72 cm/pixel) produced by the DJI Air 2S CMOS sensor allowed for the identification of distinct coral morphologies, the use of an RGB-only platform presents inherent spectral limitations. As noted by Ventura *et al.* (2023), consumer-grade RGB sensors lack the narrow-band spectral resolution required to differentiate between benthic classes with overlapping reflectance patterns, such as coral rubble and branching coral. The spectral confusion observed between these categories in this study is likely a result of these broadband constraints.

Furthermore, the current methodology did not implement a dedicated water-column correction, which is critical for mitigating the effects of light attenuation in shallow marine environments. Light reaching the sensor is significantly altered by water depth and turbidity, which can homogenize the spectral signatures of different substrates. Although radiometric consistency was partially managed through Structure-from-Motion (SfM) photogrammetry and specific flight timing to minimize sun glint, RGB sensors remain sensitive to fluctuating atmospheric conditions. To improve the reliability of future monitoring, it is recommended to transition to multispectral or hyperspectral platforms. These sensors provide the high radiometric fidelity and additional spectral bands (e.g., red-edge and NIR) necessary to account for water column effects and enhance the characterization of heterogeneous reef systems.

### CONCLUSION

This research establishes a robust, high-spatial-fidelity baseline for the marine ecosystems at Mantanani Besar Island. By quantifying the current distribution of live coral and rubble, this study provides the necessary starting point for periodic, long-term monitoring campaigns. Such a time-series approach is essential to move beyond the current snapshot and definitively track ecological trends and the efficacy of future conservation interventions. To build upon this baseline, it is recommended that future monitoring campaigns extend UAV surveys to encompass the entire Mantanani Archipelago, thereby establishing a comprehensive ecological record. Furthermore, the long-term sustainability of the island's biodiversity depends on the implementation of stringent regulatory frameworks to mitigate sediment runoff and manage unregulated tourism. Such

measures, complemented by the establishment of marine protected areas and periodic high-resolution monitoring, will be pivotal in safeguarding Mantanani's natural heritage while fostering sustainable eco-tourism practices.

## ACKNOWLEDGEMENTS

The authors would like to thank the Sabah Biodiversity Centre (SaBC) for providing the research permit (Licence No. JKM/MBS.1000-2/2 JLD.21 (29)). The Universiti Malaysia Sabah (UMS) funded and supported this research through the Coastal Connections Living Lab grant (DLV2403), and the reporting was done under a Memorandum of Understanding (MoU) between UMS and JSK Mantanani Island Resorts Sdn. Bhd. We would also like to thank the JSK Mantanani Island Resorts team for their logistical support, hospitality, and assistance during the field data collection phase of this study.

## REFERENCES

- [1] Andréfouët, S., Muller-Karger, F. E., Hochberg, E. J., Hu, C. & Carder, K. L. 2001. Change detection in shallow coral reef environments using Landsat 7 ETM + data. *Remote Sensing of Environment*, 78(1–2), 150–162.
- [2] Burdziakowski, P. & Bobkowska, K. 2021. UAV photogrammetry under poor lighting conditions—Accuracy considerations. *Sensors*, 21(10), 3531.
- [3] Casella, E., Rovere, A., Pedroncini, A., Stark, C. P., Casella, M., Ferrari, M. & Firpo, M. 2016. Drones as tools for monitoring beach topography changes in the Ligurian Sea (NW Mediterranean). *Geo-Marine Letters*, 36(2), 151–163.
- [4] Casella, E., Collin, A., Harris, D., Ferse, S., Bejarano, S., Parravicini, V., Hench, J. L. & Rovere, A. 2017. Mapping coral reefs using consumer-grade drones and structure from motion photogrammetry techniques. *Coral Reefs*, 36(1), 269–275.
- [5] Castellanos-Galindo, G. A., Casella, E., Mejía-Rentería, J. C. & Rovere, A. 2019. Habitat mapping of remote coasts: Evaluating the usefulness of lightweight unmanned aerial vehicles for conservation and monitoring. *Biological Conservation*, 239, 108282.
- [6] Chong, W. S., Zaki, N. H. M., Hossain, M. S., Muslim, A. M. & Pour, A. B. 2021. Introducing Theil-Sen estimator for sun glint correction of UAV data for coral mapping. *Geocarto International*, 37(15), 4527–4556.
- [7] Chong, W. S., Khodzori, F. A. & Shah, M. D. 2023. The Synergy of Remote Sensing in Marine Invasion Science. In: Shah, M. D., Ransangan, J. & Venmathi Maran, B. A. (Eds.). *Marine Biotechnology: Applications in Food, Drugs and Energy*. Singapore: Springer Nature Singapore. pp. 299–313.
- [8] Colomina, I. & Molina, P. 2014. Unmanned aerial systems for photogrammetry and remote sensing: A review. *ISPRS Journal of Photogrammetry and Remote Sensing*, 92, 79–97.
- [9] Green, E. P., Mumby, P. J., Edwards, A. J. & Clark, C. D. 2000. *Remote Sensing Handbook for Tropical Coastal Management*. Coastal Management Sourcebooks 3.
- [10] Hamylton, S. 2011. Estimating the coverage of coral reef benthic communities from airborne hyperspectral remote sensing data: Multiple discriminant function analysis and linear spectral unmixing. *International Journal of Remote Sensing*, 32(24), 9673–9690.
- [11] Hughes, T. P., Kerry, J. T., Baird, A. H., Connolly, S. R., Dietzel, A., Eakin, C. M., Heron, S. F., Hoey, A. S., Hoogenboom, M. O., Liu, G., Stella, J. S. & Torda, G. 2018a. Global warming transforms coral reef assemblages. *Nature*, 556(7702), 492–496.

- [12] Hughes, T. P., Anderson, K. D., Connolly, S. R., Heron, S. F., Kerry, J. T., Lough, J. M., Baird, A. H., Baum, J. K., Berumen, M. L., Bridge, T. C., Torda, G. & Wilson, S. K. 2018b. Spatial and temporal patterns of mass bleaching of corals in the Anthropocene. *Science*, 359(6371), 80–83.
- [13] Meister, M. & Qu, J. J. 2024. Quantifying Seagrass Density Using Sentinel-2 Data and Machine Learning. *Remote Sensing*, 16(7), 1165.
- [14] Mumby, P. J., Green, E. P., Edwards, A. J. & Clark, C. D. 1999. The cost-effectiveness of remote sensing for tropical coastal resources assessment and management. *Journal of Environmental Management*, 55(3), 157–166.
- [15] Muslim, A. M., Chong, W. S., Safuan, C. D. M., Khalil, I. & Mohammad Shawkat Hossain. 2019. Coral reef mapping of UAV: A comparison of sun glint correction methods. *Remote Sensing*, 11(20), 2422.
- [16] Pajares, G. 2015. Overview and Current Status of Remote Sensing Applications Based on Unmanned Aerial Vehicles (UAVs). *Photogrammetric Engineering & Remote Sensing*, 81(4), 281–330.
- [17] Stone, A., Hickey, S., Radford, B. & Wakeford, M. 2024. Mapping emergent coral reefs: a comparison of pixel-and object-based methods. *Remote Sensing in Ecology and Conservation*, 11, 20-39.
- [18] Tuttle, L. J. & Donahue, M. J. 2022. Effects of sediment exposure on corals: a systematic review of experimental studies. *Environmental Evidence*, 11(1), 4.
- [19] Ventura, D., Grosso, L., Pensa, D., Casoli, E., Mancini, G., Valente, T., Scardi, M. & Rakaj, A. 2023. Coastal benthic habitat mapping and monitoring by integrating aerial and water surface low-cost drones. *Frontiers in Marine Science*, 9, 1096594.
- [20] Wilkinson, C. R. 2008. *Status of coral reefs of the world*. Global Coral Reef Monitoring Network and Reef and Rainforest Research Center.
- [21] Wu, M. T. 2022. Confusion matrix and minimum cross-entropy metrics based motion recognition system in the classroom. *Scientific Reports*, 12(1), 3095.